Published in final edited form as:
Stem Cells. 2007 October ; 25(10): 2677–2684. doi:10.1634/stemcells.2007-0041.

Molecular Imaging of Bone Marrow Mononuclear Cell Homing and Engraftment in Ischemic Myocardium

Ahmad Y. Sheikh, MD[*,1], **Shu-An Lin, MS**[*,2], **Feng Cao, MD, PhD**[2], **Yuan Cao, PhD**[2], **Koen E.A. van der Bogt**[1], **Pauline Chu, BS**[3], **Ching-Pin Chang, MD, PhD**[4], **Christopher H. Contag, PhD**[2], **Robert C. Robbins, MD**[1], and **Joseph C. Wu, MD, PhD**[2,4]

[1]Department of Cardiothoracic Surgery, Stanford Stanford University School of Medicine, Stanford, CA, USA

[2] Molecular Imaging Program at Stanford (MIPS) Stanford University School of Medicine, Stanford, CA, USA

[3]Department of Comparative Medicine Stanford University School of Medicine, Stanford, CA, USA

[4]Department of Medicine, Division of Cardiology. Stanford University School of Medicine, Stanford, CA, USA

Abstract

Bone marrow mononuclear cell (BMMC) therapy shows promise as a treatment for ischemic heart disease. However, the ability to monitor long-term cell fate remains limited. We hypothesize molecular imaging can be used to track stem cell homing and survival after myocardial ischemia-reperfusion (I/R) injury. We first harvested donor BMMCs from adult male L2G85 transgenic mice constitutively expressing both firefly luciferase (Fluc) and enhanced green fluorescence protein (eGFP) reporter gene. FACS analysis revealed ~0.07% of the population to consist of classical hematopoietic stem cells (lin-, thy-int, c-kit+, Sca-1+). Afterwards, adult female FVB recipients (n=38) were randomized to sham surgery or acute I/R injury. Animals in the sham (n=16) and I/R (n=22) groups received 5×10^6 of the L2G85-derived BMMCs via tail vein injection. Bioluminescence imaging (BLI) was used to track cell migration and survival *in vivo* for 4 weeks. BLI showed preferential homing of BMMCs to hearts with I/R injury compared to sham hearts within the first week following cell injection. *Ex vivo* analysis of explanted hearts by histology confirmed BLI imaging results, and quantitative RT-PCR (for the male *Sry* gene) further demonstrated higher number of BMMCs in hearts with I/R injury compared to the sham group. Functional evaluation by echocardiography demonstrated a trend towards improved left ventricular fractional shortening in animals receiving BMMCs. Taken together, these data demonstrate that molecular imaging can be used to successfully track BMMC therapy in murine models of heart disease. Specifically, we demonstrate that systemically delivered BMMCs preferentially home to and are retained by injured myocardium.

Keywords

heart diseases; bone marrow; cell homing; molecular imaging

Correspondence to: Joseph C. Wu, MD, PhD, Stanford University School of Medicine, Edwards Building R354, Stanford, CA 94305-5344, Ph: 650-736-2246, Fax: 650-736-0234, joewu@stanford.edu.
*Contributed equally to this work.

CONFLICT OF INTERESTS: The authors declare that they have no conflicts to disclose.

INTRODUCTION

Ischemic heart disease is the leading cause of morbidity and mortality in most industrial nations. Recent animal studies[1, 2] and clinical trials[3–5] have shown that transplantation of bone marrow mononuclear cells (BMMCs) may improve heart function. Subsequently, it has been proposed that stem cells can release angiogenic factors, protect cardiomyocytes from apoptotic cell death, induce proliferation of endogenous cardiomyocytes, and recruit resident cardiac stem cells[6]. However, the retention rate of exogenously administered cells within the injured heart remains low, and the mechanistic processes underlying stem cell therapy remain unclear. In this regard, understanding the post-transplant homing, survival, and proliferation responses of transplanted cells represents a critical initial step toward a better elucidation of stem cell biology and physiology in living subjects.

Postmortem histology remains the most common technique to study engrafted cell fate in animal models. With this approach, cells are typically labeled with fluorescent dye (e.g., PKH2 or CM-DiI)[7] or genetically modified to express GFP or β-galactosidase prior to transplantation for later identification by fluorescence microscopy or enzyme staining of serial tissue sections[1, 2]. However, inherent in this method are sampling error and selection bias, as different sets of animals must be sacrificed at different time points to recreate a representative pattern of longitudinal stem cell survival [8, 9]. In addition, given the significant variability of transplanted cell behavior within individual subjects, the aforementioned invasive techniques are inadequate for studying the spatiotemporal kinetics of stem cell homing and engraftment.

In this study, we hypothesize that reporter gene-based imaging can be used to study transplanted BMMC homing, survival, and engraftment in the ischemic myocardium. Using donor BMMCs from transgenic animals that constitutively express both Fluc and eGFP in all tissues[10], the biodistribution of BMMCs was tracked for 4 weeks following systemic delivery into syngeneic wild-type mice. Although there are reports investigating such survival and homing kinetics using radiolabeling[11–13] and iron particle labeling[13, 14] methodologies, those studies are limited by the inability to track long-term cell behavior *in vivo*. The technique employed in the present study offers significant advantages in this regard as we describe the homing and survival kinetics of cells up to 4 weeks following transplant.

METHODS

Animals

Adult female FVB mice (n=41, Jackson Laboratories, Bar Harbor, MN) and male L2G85 reporter transgenic mice (n=14, Contag Laboratory, Stanford, CA) were used. Transgenic animals (L2G85) were created on the FVB background to constitutively express both firefly luciferase and enhanced green fluorescence protein (Fluc-eGFP) in all tissues and organs, including bone marrow cell populations[10]. Animal care was provided in accordance with the Stanford University School of Medicine guidelines and policies for the use of laboratory animals.

Study Design

Female FVB mice were mechanically ventilated with 2–3% isoflurane and 100% O_2. Animals were randomized into two groups: **(a)** I/R injury (n=24) by occlusion of left anterior descending (LAD) coronary artery for 30 minutes and (**b**) sham procedure with open thoracotomy and suture around LAD but no occlusion (n=17). Surgery was performed by a single experienced surgeon (AYS). Three hours following surgery, I/R animals (n=17)

received 5×10^6 BMMCs (harvested from male L2G85 transgenic donors) via tail vein injection. A subset of the I/R animals (n=5) received 100 μl of PBS via tail vein to serve as controls for functional echocardiography study. Cell therapy was monitored by optical bioluminescence imaging (BLI) on days 1, 2, 4, 6, 8, 10, 14, 21, and 28, using D-Luciferin (300 mg/g body weight, intraperitoneal) as the reporter probe[15]. BLI results were validated by *ex vivo* by histological evaluation and RT-PCR analysis for the male *Sry* gene. Echocardiography was performed pre-operatively and at 1 and 4 weeks post-operatively to determine functional improvement in animals that received BMMCs compared to those that received PBS.

Preparation of Bone Marrow Mononuclear Cells (BMMC)

Bone marrow cells were harvested from the long bones of male L2G85 transgenic mice and isolated by centrifugation in a density cell separation medium (Ficoll-Hypaque) prior to cardiac injection[3].

Flow Cytometry Analysis

1×10^6 BMMCs were incubated in 2% FBS/PBS at 4°C for 30 min with 1 μl monoclonal antibody specific for CD31, CD34, CD45, sca-1, c-kit (BD, San Jose, CA), or left unstained for analysis by FACSCalibur with Cellquest software (BD, San Jose, CA).

Bioluminescence imaging of BMMC transplantation

BLI was performed using the Xenogen In Vivo Imaging System (Alameda, CA). The system consists of a super sensitive, cooled (−90°C) CCD camera mounted onto a light-tight imaging chamber. The CCD chip is 2.7 cm^2, and consists of 2048×2048 pixels at 13.5 microns each. The camera is capable of detecting a minimum radiance of 100 photons per second per centimeter square per steridian (photons/s/cm^2/sr) and can achieve a minimal image pixel resolution of 50 microns[15]. The system does not allow for 3 dimensional imaging, and hence spatial resolution is limited to a compressed, 2 dimensional image for analysis. Images were acquired using 1–10 minute intervals until peak signal was observed. BLI was quantified by creation of polygonal regions of interest (ROIs) over the precordium by a blinded operator (F.C.). For *ex vivo* cardiac imaging, hearts were explanted and immediately immersed into 5 mm culture dishes containing 2–3 mls of 12 Molar D-Luciferin in PBS. Images were acquired using a 1–2 minute interval until peak signal was observed.

Tissue fixation and immunohistochemical analysis

Following intubation, the chest was opened and the heart perfusion fixed for 2 minutes at 120 mmHg with 4% paraformaldehyde (Sigma, St. Louis, Mo) in phosphate buffered saline (PBS) via left ventricular stab (a right atrial defect provided the egress for blood and fluid). Fixed hearts were immersed in 30% sucrose overnight, embedded into OCT, frozen, and prepared into 10-micron thick frozen sections. Anti-GFP (rabbit polyclonal conjugated to Alexa Fluor 488 (Invitrogen, Carlsbad, CA) and rabbit polyclonal anti-troponin I (Santa Cruz Biotehcnology) staining was carried out. Primary antibodies were used at dilutions of 1:200 (anti-GFP) and 1:100 (anti-troponin I). Secondary biotinylated anti-rabbit antibody (Invitrogen) was used for troponin-I and visualized with streptavidin Alexa Fluor 555 (Invitrogen). Confocal microscopy was performed on a Leica SP5 confocal system (Leica, Wetzlar, Germany).

Ex vivo quantification of intra-cardiac surviving BMMCs

For *ex vivo* validation of BLI, a standard curve was first generated by correlating (1) cycle counts from real-time polymerase chain reaction (RT-PCR) probing for the Sry gene with

(2) known numbers of male BMMCs injected into female hearts. Specifically, 10 female hearts from WT animals were excised and immediately injected with known amounts of male BMMCs ranging from 100 to 1×10^7 cells. Whole heart DNA was then isolated using DNAzol reagent (Invitrogen, Carlsbad, CA) according to the manufacturer's protocol. Real-time polymerase chain reaction (RT-PCR) was performed on a 7900HT Sequence Detection System with TaqMan Assays on Demand gene expression probes (systems and probe from Applied Biosystems, Foster City, CA) for the SRY gene (Mm00441712_s1). Hearts were then collected from experimental animals (shams; n=11 and I/R; n=11) at day 2 and week 2 post-operatively, followed by DNA extraction and RT-PCR for SRY. Cycle count results were fit to the equation generated by the standard curve in order to determine number of male cells present in each sample.

Echocardiographic Determination of Left Ventricular Contractility

Echocardiography was performed using the General Electric Vivid 7 Dimension imaging system equipped with a 13 MHz linear probe (GE, Milwaukee, MI). Mice were assessed pre-operatively, weekly there after post-BMMC or PBS infusion. Animals were induced with isoflurane and received continuous inhaled anesthetic (1.5–2%) for the duration of the imaging session and imaged in the supine position. Echocardiography was performed by an independent operator (FC) blinded to the study conditions. M-mode short axis views of the LV were obtained and archived. Analysis of the M-Mode images was performed using GE built-in analysis software. Left ventricular end diastolic diameter (EDD) and end-systolic diameter (ESD) were measured and used to calculate fractional shortening (FS) by the following formula: FS= [EDD-ESD]/EDD[16].

Statistical Analysis

Experimental results are expressed as mean ± SEM. Linear regression analysis was performed to determine correlation between 2 variables. Repeated measures ANOVA with post-hoc testing and non-paired Student's T-test were used where appropriate. The level of significance was set at $P < 0.05$.

RESULTS

Flow cytometry analysis of BMMCs

In order to understand the characteristics of BMMCs isolated from L2G85 transgenic mice, we analyzed their cell surface markers. Based on the average of 3 FACS analysis, ~41% of BMMCs expressed CD31, an endothelial cell marker (Figure 1A); ~28% expressed stem cell marker c-kit, which is present on hematopoietic stem cells (HSCs) and mesenchymal stem cells (MSCs) (Figure 1B)[17]; ~99% expressed CD45, a hematopoietic and leukocyte marker (Figure 1C); ~16% expressed stem cell antigen-1 (Sca-1) marker (Figure 1D); ~10% expressed CD34, a myeloid progenitor cell antigen that is also present in endothelial cells and some fibroblasts (Figure 1E)[18]; and ~4.5% co-expressed both c-kit and Sca-1 (Figure 1F). Expression of c-kit and Sca-1 was reciprocal; however, when the lineage marker-negative (Lin^-) population was gated, the c-kit and Sca-1 double-positive fraction was approximately 0.07% of the bone marrow, representing the “classical” HSC population as described by Okada and colleagues[17]. Overall, the surface marker patterns of L2G-derived BMMCs were consistent with those used in clinical trials[3–5].

Linear correlation between cell numbers versus *ex vivo* BLI signals or *in vitro* enzyme assay

The L2G85 mice constitutively express both Fluc and eGFP reporter genes in all tissues and organs, including harvested bone marrow cell populations[10]. Representative

bioluminescence images of BMMCs are shown in Figure 2A. *Ex vivo* analysis showed a linear relationship between cell number versus BLI signal (R^2=0.99) as well as cell number versus Fluc enzyme activity (R^2=0.99) (Figure 2B). These data suggest that BLI of Fluc reporter gene can be used to accurately follow and quantify transplanted stem cells in small living animals. Fluorescence microscopy of BMMN cells demonstrated uniform eGFP expression within the cytosol (Figure 2C). FACS analysis demonstrated over 87% of the BMMN fraction strongly expressed eGFP as shown in Figure 2D.

Tracking BMMC fate in living mice by *in vivo* BLI

To assess homing and biodistribution, noninvasive imaging was performed on days 1, 2, 4, 6, 8, 10, 14, 21, and 28 (Figure 3). ROIs were created over the precordium and average radiance was measured. For the sham group, Fluc imaging signals were $1.92\pm0.01\times10^3$ photons/sec/cm^2/sr on day 1, $3.51\pm0.11\times10^3$ on day 2, $6.29\pm0.93\times10^3$ on day 4, $7.19\pm0.22\times10^3$ on day 6, $6.86\pm0.78\times10^3$ on day 8, $4.97\pm0.22\times10^3$ on day 10, $4.10\pm0.97\times10^3$ on day 14, $3.77\pm0.53\times10^3$ on day 18, $3.62\pm0.36\times10^3$ on day 21, and $3.55\pm0.13\times10^3$ on day 28 (Figure 3). Background imaging signal (taken from ROIs created upon control non-recipient animals [n=5] given only D-Luciferin) ranged between 1.5×10^3 to 3.5×10^3 photons/sec/cm^2/sr. Migration of BMMCs to lung, spleen, and femurs could be visualized in both groups. Quantitative analysis also showed that the I/R group had significantly stronger chest Fluc activities at day 2 and day 6 compared to the sham group (P<0.01) (Figure 4A). As animals in both groups received lateral thoracotomy, the higher imaging signals in the I/R group indicates that more BMMCs are homing to the acutely injured hearts compared to the normal hearts. We further confirmed this observation by *ex vivo* imaging of explanted whole hearts on day 2 following BMMC transplant (Figure 4B). Interestingly, the largest differences in signal activity between I/R and sham were observed within the first 10 days following transplantation, suggesting increased homing, proliferation, and/or retention within the ischemic myocardium during this period. Overall, the sham animals were also noted to have a relatively high signal compared to expected background levels from an unoperated mouse. This effect is most likely explained by the thoracotemy itself, as the inflammatory insult provided by the surgical wound serves as a stimulus for BMMC homing and retention.

Histological evaluation of BMMC homing to the heart

Fluorescence microscopy revealed clear evidence of $eGFP^+$ BMMC homing to the injured heart, and further validated our BLI measurements. In keeping with the native, post-infarct inflammatory response, transplanted cells were observed in the infarct border zones (Figure 5A & 5B). Confocal laser microscopy confirmed the presence of transplanted cells within the myocardium 2 days following delivery (Figure 5C).

Ex vivo confirmation of BMMC homing into ischemic myocardium by probing *Sry* gene

The *Sry* gene, a target DNA sequence located in the motif of Y-linked testis-determination gene, was originally amplified to study human sex determination at the single cell level[19]. Since this test is highly precise, it has been adapted to monitor the clinical outcome of allogeneic hematopoietic transplantation[20] as well as animal study focused on cardiac stem cell therapy[21]. In order to confirm our imaging results of cell homing, we first established a correlation between RT-PCR (Taqman) amplification cycle number to injected BMMC number by probing *Sry* gene from freshly isolated female heart samples directly injected (*ex vivo*) with known numbers of male BMMCs. Figure 6A shows the robust correlation between BMMC number and cycle number of real-time PCR (r^2=0.99) using this approach. The *Sry* gene test was then performed on hearts harvested from our experimental animals at different time points following BMMC injection. Quantitative real-time PCR showed significantly more BMMCs homed in to the myocardium in the I/R group compared to sham

group on day 2 (245±68 vs. 2580±421 $P<0.01$), consistent with our *in vivo* imaging analysis (Figure 6B). There was also a trend for increased BMMC numbers in the I/R group at week 2 (1540±470 vs. 2796±585), but this did not reach statistical significance ($P=0.078$).

Assessment of cardiac function by echocardiography

In order to determine whether intravenously delivered BMMCs improved cardiac contractiltiy, we performed echocardiography pre-operatively and weekly post-operatively. Representative M-mode images of mice injected with PBS as control or BMMCs at week 4 are shown in Figure 7A. At 1 week, fractional shortening decreased comparably in both groups. By 4 weeks, there was a trend toward better functional improvement in the BMMC group compared to control PBS group (38.5±1.8% vs. 35.2±1.3%), but this did not reach statistical significance (Figure 7B). Data from intermittent assessment of FS between weeks 1 and 4 demonstrated a similar, non significant trend and are not shown on the graph to preserve clarity.

DISCUSSION

In this study, we present evidence that reporter gene imaging can be used to track BMMC homing, retention, and survival in a mouse model of acute cardiac ischemia and reperfusion (I/R) injury. Our data can be summarized as follows: (1) the existence of a robust correlation between cell numbers and reporter gene imaging signals; (2) preferential homing of BMMCs within the first week of I/R injury; (3) <0.1% of the total BMMCs delivered eventually engrafted into the heart by two weeks after intravenous delivery; and (4) intravenous delivery of BMMCs did not confer significant improvement of ischemia-induced left ventricular contractility.

The success of stem cell therapy will likely require novel methods to determine the dynamic biodistribution and long-term fate of transplanted cells without reliance on postmortem histology. In recent years, several imaging techniques have been developed to better understand stem cell fate *in vivo*. In general, they can be divided into two broad methodologies: direct labeling and indirect reporter gene-based imaging[8, 9]. The former uses a detectable probe (e.g., radioactivity or iron particles) that can be loaded into cells prior to delivery. Aicher *et al.* first demonstrated tissue distribution of endothelial progenitor cells incubated with radioactive [^{111}In]-oxine could be successfully monitored by scintigraphic imaging[11]. As [^{111}In]-oxine has a half-life of 67.3 hours, only ~2% of the radioactivity remained in the infarcted heart after 96 hours. A follow-up study by Kraitchman *et al.* injected porcine mesenchymal stem cells labeled with [^{111}In]-oxine intravenously and showed cardiac engraftment up to 7 days by single photon emission computed tomography (SPECT)[13]. More recently, Hoffman *et al.* injected human bone marrow cells labeled with 2-[18F]-fluoro-2-deoxy-D-glucose ([^{18}F]-FDG) via both intracoronary and intravenous routes[12]. Since [^{18}F]-FDG has a half-life of 110 minutes, positron emission tomography (PET) imaging needed to be performed *within* 2 hours after cell delivery. The authors observed 1.3% to 2.6% of [^{18}F]-FDG-labeled bone marrow cells present in the myocardium after intracoronary delivery and, interestingly, only background activity was detected after intravenous delivery. Taken together, these studies suggest that radiolabeling techniques are suitable for immediate, short-term tracking of delivered cells but less apt for long-term follow-up[8, 9].

In contrast to the short half-life of radioactive probes, iron oxide particles can be tracked for long periods of time. Amado *et al.* showed that porcine mesenchymal stem cells labeled with Feridex can be delivered by endomyocardial injection and tracked by magnetic resonance imaging (MRI) for 8 weeks[14]. However, the main limitation of such direct iron-labeling techniques is that the MRI signals do *not* necessarily reflect cell viability, because the iron

particles might persist within dead cells, leak into intercellular space, and/or be engulfed by resident macrophages[22]. These factors might explain why quantitative analysis of the iron-labeled retention showed >40% of the iron-labeled mesenchymal stem cells were still present 8 weeks after delivery in the study by Amado and colleagues[14]. Indeed, it is well recognized that adult stem cells have poor post-transplant viability with an estimated 99% of mesenchymal stem cells dying within 4 days after injection into healthy mouse hearts[23].

Notwithstanding the technical limitations of the aforementioned direct imaging techniques, the ideal cellular imaging platform should provide information regarding the following: (i) real-time, dynamic cell biodistribution kinetics; (ii) long-term cell survival; and (iii) rates of cellular proliferation. At present, both methodologies described above lack these characteristics. An alternative approach--reporter gene imaging--is playing an increasingly prominent role in monitoring stem cell fate as demonstrated by this study and other studies reviewed elsewhere[8, 9]. Because reporter genes are DNA sequences that encode for reporter proteins, one can follow the signal for as long as the transplanted cells and their progeny are viable. If, for example, the stem cells are dead or apoptotic, there will be no transcription and translation of the reporter gene, and thus no imaging signal. Similarly, if cells are actively migrating away from a particular ROI, signal strength will also decrease. Likewise, if the transplanted stem cells proliferate *in vivo*, or migrate into a particular ROI, there will be an increase in the imaging signal detected from that area. Using this elegant reporter gene approach, we have been able to monitor BMMC homing over a relatively protracted time period (compared to radiolabeling technique[11–13]) as well as to quantify BMMC survival more accurately (compared to iron labeling technique[14, 22]). However, the low energy photons (2–3 eV) from BLI can become attenuated within deeper tissues (e.g., heart) compared to more superficial locations (e.g., skeletal muscles). In our experience, the lower detection limit of BMMCs within the heart is approximately on the order of 1,000 cells compared to 100 cells in the subcutaneous tissue over the leg (unpublished data).

In our study, bioluminescence imaging of the I/R group showed significantly higher cell signal activity in the heart compared to the sham group during the first week. This difference is likely due to activation of cytokines that promotes homing of BMMCs to the ischemic sites[6]. A previous study using gene expression analysis has shown that stromal cell-derived factor-1α (SDF-1), vascular endothelial growth factor (VEGF), matrix metalloproteinase-9 (MMP-9), intercellular adhesion molecule-1 (ICAM-1), and vascular cell adhesion molecule-1 (VCAM-1) are activated after myocardial infarction[24]. The exact chemoattractant factors responsible for stem cell homing remain unclear, and the process itself may be inefficient as shown by our *in vivo* imaging, histological analysis, and *ex vivo* real-time PCR. In fact, by 2 weeks following transplant, less than 0.1% of the total injected cells remained engrafted in the recipient hearts. The low number of cell engraftment may also explain the lack of improvement in cardiac function observed in our study. It is possible that the observed trend might have achieved statistical significance with a larger cohort of animals. Moreover, our study remains limited in that we did not follow animals out for longer than 4 weeks to observe whether the trend in functional improvement persisted or diminished. Critical evaluation of functional improvement as a function of cell dosage and time remains an area that requires further study.

In future studies, we believe *in vitro* identification (e.g., by transcriptional profiling) and *in vivo* validation (e.g., by reporter gene imaging) of factors important to homing and cell retention will be an attractive approach to coax exogenously administered stem cells to home in to the heart and promote long-term functional improvement. However, one of the main drawbacks of bioluminescence imaging is its restriction to small animal pre-clinical validation studies, because the low-energy photons (2–3 eV) become attenuated and scattered within deep tissues[25]. In addition, the inability to perform 3-D BLI impairs ability

to accurately localize signal sources from deep tissues (e.g., heart) as discussed earlier. Specifically, one of the resultant challenges from compressing 3-D data into a 2-D picture is that of increased noise to signal ratio. In the chest, for example, the summation of lung background might obscure a relatively low cell signal emitted from the heart and measured through an ROI designated over a two dimensional space. Thus, ongoing development of positron emission tomography (PET)-based reporter gene and reporter probe technique that uses high-energy photons (511 keV) and have 3-D imaging capabilities will be necessary for clinical application in the future[26].

In conclusion, our study suggests that reporter gene imaging can be a valuable tool for studying stem cell fate *in vivo*. The same imaging platform can be adopted to investigate basic mechanisms underlying myocardial cell therapy and optimize the key variables involved, such as the most efficacious cell type(s), appropriate cell dosing, and best routes of delivery (e.g., intracoronary versus intravenous). We hope that carefully designed studies using the reporter gene imaging techniques developed here and in future investigations will lead not only to advancement of stem cell research, but also to useful novel therapies and diagnostic tools for clinicians and patients.

Acknowledgments

This work was supported in part by grants from the AHA, ACCF/GE, ASNC (JCW), NHLBI (JCW, AYS), and SNM Student Fellowship (SL).

REFERENCE

1. Orlic D, Kajstura J, Chimenti S, et al. Bone marrow cells regenerate infarcted myocardium. Nature. Apr 5; 2001 410(6829):701–705. [PubMed: 11287958]
2. Yoon YS, Wecker A, Heyd L, et al. Clonally expanded novel multipotent stem cells from human bone marrow regenerate myocardium after myocardial infarction. J Clin Invest. Feb; 2005 115(2): 326–338. [PubMed: 15690083]
3. Perin EC, Dohmann HF, Borojevic R, et al. Improved exercise capacity and ischemia 6 and 12 months after transendocardial injection of autologous bone marrow mononuclear cells for ischemic cardiomyopathy. Circulation. Sep 14; 2004 110(11 Suppl 1):II213–218. [PubMed: 15364865]
4. Strauer BE, Brehm M, Zeus T, et al. Repair of infarcted myocardium by autologous intracoronary mononuclear bone marrow cell transplantation in humans. Circulation. Oct 8; 2002 106(15):1913–1918. [PubMed: 12370212]
5. Wollert KC, Meyer GP, Lotz J, et al. Intracoronary autologous bone-marrow cell transfer after myocardial infarction: the BOOST randomised controlled clinical trial. Lancet. Jul 10; 2004 364(9429):141–148. [PubMed: 15246726]
6. Wollert KC, Drexler H. Clinical applications of stem cells for the heart. Circ Res. Feb 4; 2005 96(2):151–163. [PubMed: 15692093]
7. Barbash IM, Chouraqui P, Baron J, et al. Systemic delivery of bone marrow-derived mesenchymal stem cells to the infarcted myocardium: feasibility, cell migration, and body distribution. Circulation. Aug 19; 2003 108(7):863–868. [PubMed: 12900340]
8. Sheikh AY, Wu JC. Molecular imaging of cardiac stem cell transplantation. Curr Cardiol Rep. Mar; 2006 8(2):147–154. [PubMed: 16524542]
9. Zhou R, Acton PD, Ferrari VA. Imaging stem cells implanted in infarcted myocardium. J Am Coll Cardiol. Nov 21; 2006 48(10):2094–2106. [PubMed: 17112999]
10. Cao YA, Wagers AJ, Beilhack A, et al. Shifting foci of hematopoiesis during reconstitution from single stem cells. Proc Natl Acad Sci U S A. Jan 6; 2004 101(1):221–226. [PubMed: 14688412]
11. Aicher A, Brenner W, Zuhayra M, et al. Assessment of the tissue distribution of transplanted human endothelial progenitor cells by radioactive labeling. Circulation. Apr 29; 2003 107(16): 2134–2139. [PubMed: 12695305]

12. Hofmann M, Wollert KC, Meyer GP, et al. Monitoring of bone marrow cell homing into the infarcted human myocardium. Circulation. May 3; 2005 111(17):2198–2202. [PubMed: 15851598]

13. Kraitchman DL, Tatsumi M, Gilson WD, et al. Dynamic imaging of allogeneic mesenchymal stem cells trafficking to myocardial infarction. Circulation. Sep 6; 2005 112(10):1451–1461. [PubMed: 16129797]

14. Amado LC, Saliaris AP, Schuleri KH, et al. Cardiac repair with intramyocardial injection of allogeneic mesenchymal stem cells after myocardial infarction. Proc Natl Acad Sci U S A. Aug 9; 2005 102(32):11474–11479. [PubMed: 16061805]

15. Cao F, Lin S, Xie X, et al. In vivo visualization of embryonic stem cell survival, proliferation, and migration after cardiac delivery. Circulation. Feb 21; 2006 113(7):1005–1014. [PubMed: 16476845]

16. Collins KA, Korcarz CE, Lang RM. Use of echocardiography for the phenotypic assessment of genetically altered mice. Physiol Genomics. May 13; 2003 13(3):227–239. [PubMed: 12746467]

17. Okada S, Nakauchi H, Nagayoshi K, Nishikawa S, Miura Y, Suda T. In vivo and in vitro stem cell function of c-kit- and Sca-1-positive murine hematopoietic cells. Blood. Dec 15; 1992 80(12): 3044–3050. [PubMed: 1281687]

18. Shi Q, Rafii S, Wu MH, et al. Evidence for circulating bone marrow-derived endothelial cells. Blood. Jul 15; 1998 92(2):362–367. [PubMed: 9657732]

19. Cui KH, Warnes GM, Jeffrey R, Matthews CD. Sex determination of preimplantation embryos by human testis-determining-gene amplification. Lancet. Jan 8; 1994 343(8889):79–82. [PubMed: 7903778]

20. Wang LJ, Chou P, Gonzalez-Ryan L, Huang W, Haut PR, Kletzel M. Evaluation of mixed hematopoietic chimerism in pediatric patients with leukemia after allogeneic stem cell transplantation by quantitative PCR analysis of variable number of tandem repeat and testis determination gene. Bone Marrow Transplant. Jan; 2002 29(1):51–56. [PubMed: 11840144]

21. Muller-Ehmsen J, Whittaker P, Kloner RA, et al. Survival and development of neonatal rat cardiomyocytes transplanted into adult myocardium. J Mol Cell Cardiol. Feb; 2002 34(2):107–116. [PubMed: 11851351]

22. Bulte JW, Kraitchman DL. Iron oxide MR contrast agents for molecular and cellular imaging. NMR Biomed. Nov; 2004 17(7):484–499. [PubMed: 15526347]

23. Toma C, Pittenger MF, Cahill KS, Byrne BJ, Kessler PD. Human mesenchymal stem cells differentiate to a cardiomyocyte phenotype in the adult murine heart. Circulation. Jan 1; 2002 105(1):93–98. [PubMed: 11772882]

24. Abbott JD, Huang Y, Liu D, Hickey R, Krause DS, Giordano FJ. Stromal cell-derived factor-1alpha plays a critical role in stem cell recruitment to the heart after myocardial infarction but is not sufficient to induce homing in the absence of injury. Circulation. Nov 23; 2004 110(21): 3300–3305. [PubMed: 15533866]

25. Contag PR, Olomu IN, Stevenson DK, Contag CH. Bioluminescent indicators in living mammals. Nature Medicine. 1998; 4(2):245–247.

26. Penuelas I, Mazzolini G, Boan JF, et al. Positron emission tomography imaging of adenoviral-mediated transgene expression in liver cancer patients. Gastroenterology. Jun; 2005 128(7):1787–1795. [PubMed: 15940613]

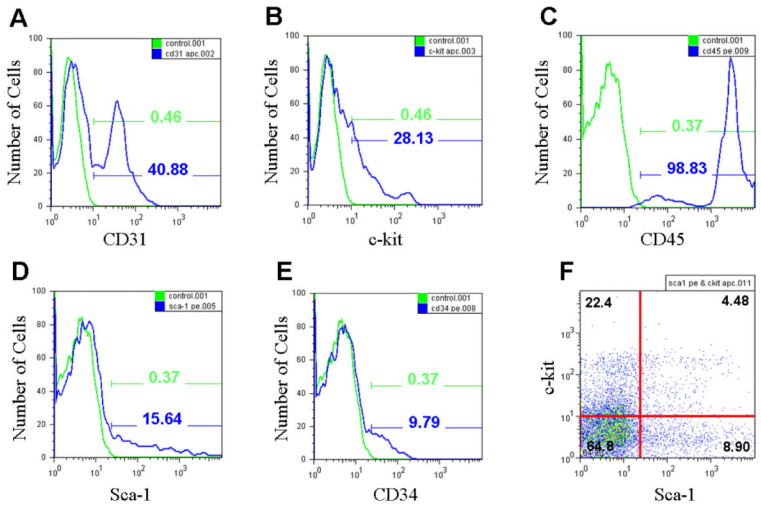

Figure 1.

FACS analysis of bone marrow mononuclear cells (BMMCs) from L2G85 transgenic reporter mice reveals typical proportions of progenitor cells for the FVB strain. Green curves with corresponding percentages representing BMMC samples labeled with (**A**) CD31, (**B**) c-kit, (**C**) CD45, (**D**) Sca-1, and (**E**) CD34. Blue curves and percentages demonstrate negative controls (no antibody). (**F**) Approximately 4.5% of the BMMCs stain positive for both c-kit and Sca-1, similar to preparations used in clinical studies of BMMC transplantation in humans.

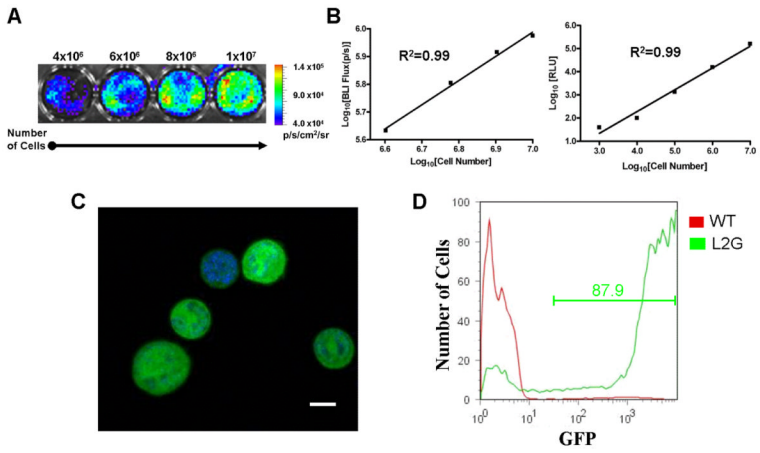

Figure 2.

Reporter gene activity correlates robustly with cell number. (**A**) Bioluminescence imaging (BLI) of increasing numbers of BMMC *in vitro* (total cell count given above corresponding well with color scale bar representing range of signal in p/s/cm^2/sr). (**B**) Correlation of cell numbers (x-axis) with BLI signal (**left**) and Fluc enzyme activity (**right**) demonstrate linear relationships with R^2 values of 0.99. (**C**) Confocal laser microscopy of BMMCs demonstrates bright, cytosolic eGFP expression with corresponding nuclei stained blue with DAPI (scale bar = 5 μm). (**D**) FACS analysis of BMMCs from wild-type control FVB mouse (red) and L2G85 transgenic mouse (green) demonstrates robust eGFP expression by over 87% of the cells.

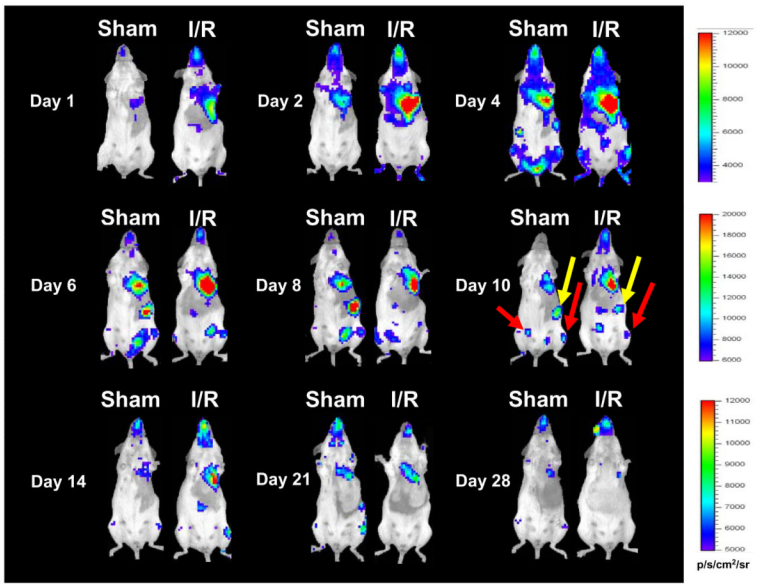

Figure 3.

Bioluminescence imaging demonstrates exogenously delivered BMMC preferentially home to injured myocardium. Images following the same animals (sham on left and I/R injury on right) for 4 weeks following intravenous delivery of L2G85-derived BMMCs (note the maximum values for scale bars in p/s/cm^2/sr are different in the three rows). Persistently elevated signal from the area overlying the heart can be observed through day 14, followed by relatively similar decreasing trend in signal intensity by day 28. Images at day 10 demonstrate entrapment of cells in extra-cardiac sites such as the spleen (yellow arrows) and long bones of the lower extremities (red arrows).

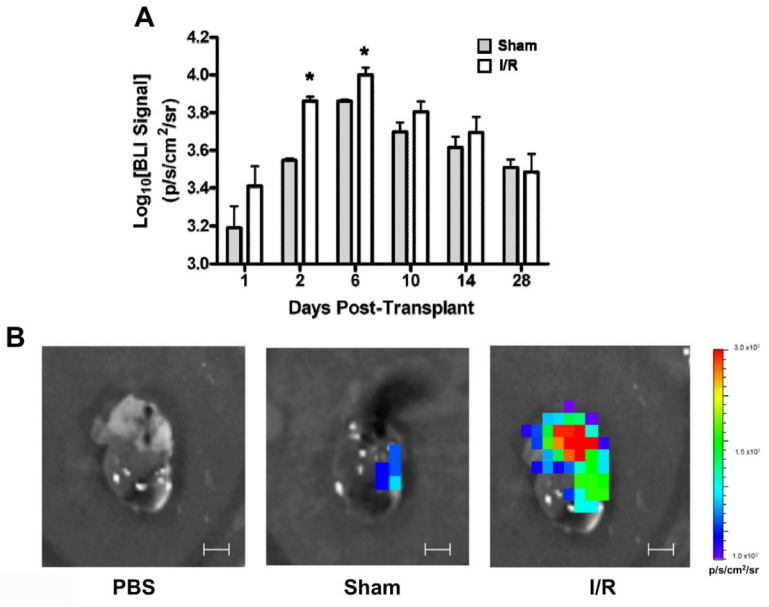

Figure 4.

Ex vivo imaging confirms presence of transplanted cells within the myocardium. (**A**) Quantification of signals from ROIs over the thorax demonstrates significantly increased cell numbers in animals with I/R injury (white bars) compared to sham (gray bars) at days 2–6 following transplant (**P*<0.05). Mean baseline Log_{10}BLI (p/s/cm^2/sr) of unoperated, uninjected mice was 3.3±2.1 (n=5 animals imaged at different time points). This was consistently 1–2 orders of magnitude lower than that of the highest signals attained in the animals receiving cells and I/R injury. (**B**) *Ex vivo* imaging of hearts two days following I/R injury with intravenous PBS (left), sham surgery with BMMCs (middle), or I/R injury with BMMCs (right) confirms homing of intravenously delivered BMMCs to the heart (white scale bars = 5 mm).

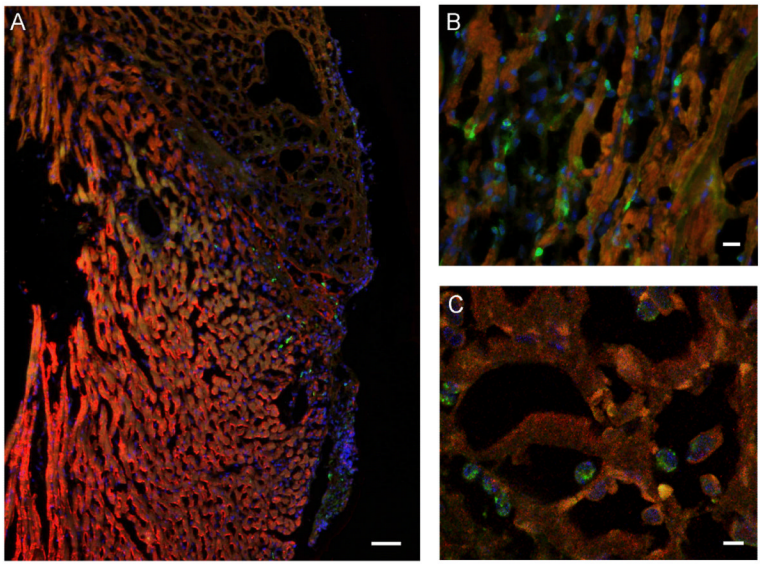

Figure 5.
Histological evaluation confirms BMMC homing to the infarcted heart. Fluorescence microscopy images of a representative heart 2 days following 30 minutes of I/R injury and injection of 5×10^6 BMMN cells via tail vein. All panels stained with anti-troponin (red), anti-GFP (green), and DAPI (blue). (**A**) Infarcted area demonstrated by lack of bright troponin stain, with numerous GFP positive cells in the infarct border zone (scale bar = 50 μm). (**B**) High-power view demonstrating numerous GFP-expressing cells within the myocardium (scale bar = 10 μm). (**C**) Confocal laser microscopy image confirming presence of GFP-expressing cells within infarcted areas of the myocardium (scale bar = 5 μm).

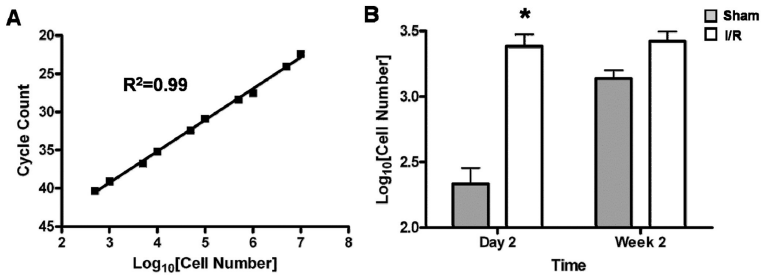

Figure 6.

Real time PCR quantification of surviving male transplanted cells within female hearts. (**A**) Plot of TaqMan-based *Sry*-quantification versus number of male cells in female hearts demonstrates a robust correlation between cycle count and known cell number (R^2=0.99). (**B**) *Ex vivo* TaqMan analysis of hearts undergoing sham surgery (grey bars) versus I/R injury (white bars) demonstrates statistically significant increase of BMMCs homing in to injured hearts compared to sham at day 2 following transplant. This trend persists at week 2, but does not achieve statistical significance (n=5–6/group) (**P*<0.05). Both results mirror findings generated by longitudinal bioluminescence imaging *in vivo* as shown in Figures 3 & 4.

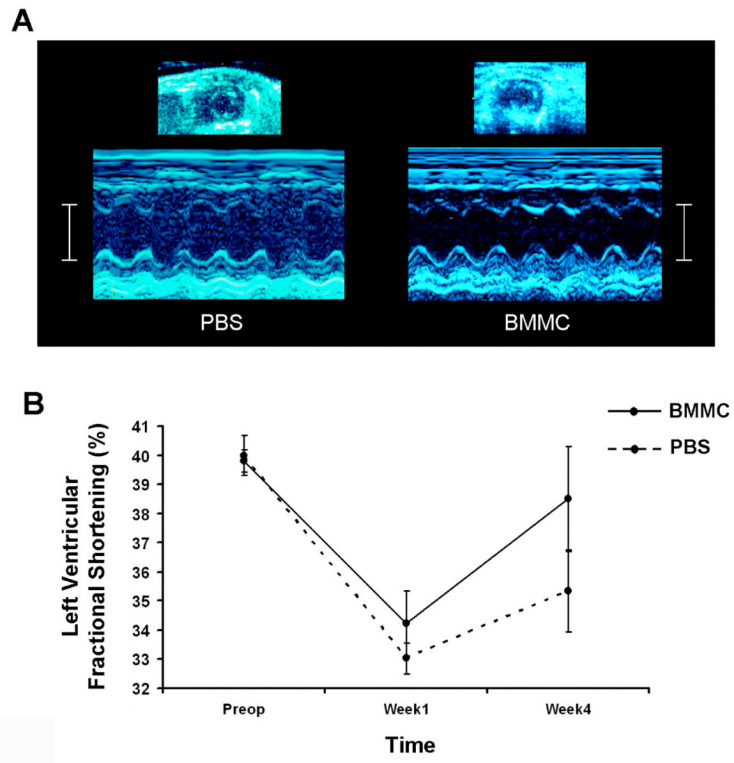

Figure 7.

Ventricular function following BMMC therapy. (**A**) Representative M-mode images of hearts at 4 weeks following I/R injury with administration of PBS (left) versus BMMCs (right) (white scale bars = 5mm). (**B**) Quantification of left ventricular function demonstrates a trend towards improved functional recovery at 4 weeks post-I/R in animals receiving BMMCs compared to PBS (n=5–6 per time point) but did not achieve statistical significance.